Available online at www.sciencedirect.com
ScienceDirect
Geomorphology 91 (2007) 302–310
GEOMORPHOLOGY
www.elsevier.com/locate/geomorph

Self-organized complexity in geomorphology: Observations and models

Donald L. Turcotte

Department of Geology, University of California, Davis, CA 95616, USA

Received 2 November 2006; accepted 30 April 2007
Available online 8 August 2007

Abstract

The focus of this paper is to relate fundamental statistical properties of landforms and drainage networks to models that have been developed in statistical physics. Relevant properties and models are reviewed and a general overview is presented. Landforms and drainage networks are clearly complex, but well-defined scaling laws are found. Coastlines, topography contours, and lakes are classic self-similar fractals. The height of topography along a linear track is well approximated as a Brownian walk, a self-affine fractal. This type of behavior has also been found in surface physics, for example the surface roughness of a fracture. An applicable model is the Langevin equation, the heat equation with a stochastic white-noise driver. This model also reproduces the statistics of sediment deposition. Drainage networks were one of the original examples of self-similar fractal trees. An important advance in quantifying the structure of drainage networks is the application of the Tokunaga fractal side-branching statistics. A classic problem in statistical physics is the diffusion-limited aggregation. The resulting tree like structures have been shown to also satisfy the Tokunaga statistics. A modified version of the diffusion-limited aggregation model reproduces the statistics of drainage networks. It is concluded that the models developed in statistical physics have direct applicability to the fundamental problems in geomorphology.

Keywords: Landforms; Drainage networks; Fractals; Diffusion-limited aggregation; Langevin equation

1. Introduction

In this paper we will discuss several aspects of the complexities associated with landforms and drainage networks (Turcotte, 2006). We first consider how these complexities are quantified. This discussion is generally carried out in terms of fractal statistics. Mandelbrot (1967) introduced the concept of fractals in terms of the length of the west coast of Great Britain. Another example of a fractal distribution in geomorphology is the frequency-area distribution of lakes. Mandelbrot (1982) also recognized that the Horton–Strahler scaling of drainage networks defined a self-similar fractal. The fractal description was subsequently extended to self-affine fractals. The three-dimensional structure of landforms is generally well represented as a self-affine fractal. This association led Mandelbrot (1982) and Voss (1989) to generate widely admired synthetic landforms. This association has also been used to interpolate well logs in order to determine the full three-dimensional sedimentary structure (Hewett, 1986, Molz et al., 2004), and in particular, to improve secondary recovery of petroleum. While fractals are certainly generally

E-mail address: turcotte@geology.ucdavis.edu.

0169-555X/$ - see front matter © 2007 Elsevier B.V. All rights reserved.
doi:10.1016/j.geomorph.2007.04.016

applicable, a fundamental question is why? Specifically, why do drainage networks exhibit a fractal scaling? To understand the scaling of drainage networks it is necessary to appreciate the importance of Tokunaga (1978) side branching. This self-similar side branching is a much better constraint on alternative models for drainage networks than the original Horton–Strahler scaling.

A model that exhibits self-similar side branching is the diffusion-limited aggregation (DLA). Ossadnik (1992) rediscovered the Tokunaga scaling and showed that the DLA clusters satisfy this scaling. DLA can also be shown to have a strong similarity to the headward migration of a drainage network into a flat plateau. A rational for this approach to fluvial landscaping has been given by Chase (1992) in terms of the random migration of "precipitons" across a landscape.

Theoretical models for surface deposition that result in the self-affine fractal scaling have been developed in the physics literature (Barabasi and Stanley, 1993). For example, solutions of the Langevin equation give this behavior. The Langevin equation is the heat equation with a white noise driver. The application of the heat equation to geomorphology was proposed by Culling (1960, 1963). It has been used to model alluvial fans and prograding river deltas. Solutions of the Langevin equation have been applied to the structure of sedimentary layering and to rates of sedimentation. In this paper we review the fractal aspects of landforms, river networks, and sedimentary layering. We also present some models that explain this behavior.

2. Fractals

Fractals are a descriptive aspect of geomorphology (landforms, drainage networks, etc.). Two important types of fractal statistics exist, the first is self-similar fractals and the second is self-affine fractals. Many times series have been shown to be self-affine fractals. Examples include $1/f$ noise and Brownian walks. Self-similar and self-affine fractals are applicable to landforms.

First, consider self-similar fractals. Several definitions exist, but the simple number-length scaling can form the basis for almost all natural applications. This can be written (Turcotte, 1997)

$$N \sim r^{-D}, \tag{1}$$

where D is the fractal dimension and N is the number of objects with a linear dimension r for a discrete distribution and the number with a linear dimension greater than r for a continuous distribution. The concept

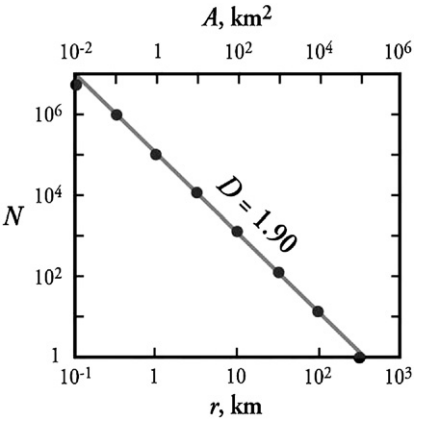

Fig. 1. Cumulative number of lakes N with areas greater than A (Meybeck, 1995). A good correlation with fractal scaling (1) is obtained taking $r=A^{1/2}$ and $D=1.90$.

of fractals was introduced in terms of the length of the west coast of Great Britain by Mandelbrot (1967). The length P of coastline has a power-law dependence on the length r of the measuring rod. Similar results are obtained for the length of topographic contours on topographic maps.

Another example of power-law (fractal) scaling is the number-area distribution of lakes as illustrated in Fig. 1 (Meybeck, 1995). The cumulative number of lakes with $r=A^{1/2}$ (A lake area) greater than a specified value is in excellent agreement with the fractal relation Eq. (1) taking $D=1.90$. This application of fractals illustrates an important feature of the fractal distribution. The applicable range of fractal statistics must have the upper and the lower bounds. The integral of the continuous fractal distribution from $r=0$ to infinity diverges. This is the reason that most statisticians reject the fractal distribution on a formal basis. Yet fractal distributions are ubiquitous in the physical and biological sciences. The fractal distribution is the only distribution that is scale invariant.

Next, we address the applicability of self-affine fractals to landforms. As a specific example we consider the height of topography along a linear track. The height of topography, δ as a function of the distance along the track L, can be considered to be a continuous time series. On average the dependence of δ on L is well approximated by (Ahnert, 1984)

$$\delta \sim L^{1/2}. \tag{2}$$

This is the standard deviation of a Brownian walk. A Brownian walk is a self-affine fractal.

Self-affine fractals can also be defined in a variety of ways, but the most widely used definition utilizes spectral

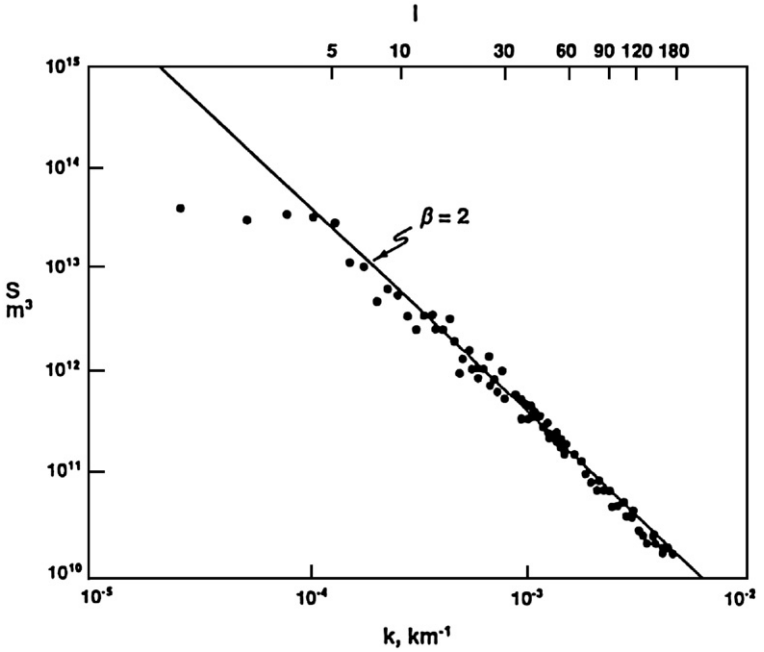

Fig. 2. Power spectral density, S, as a function of wave number, k, for a spherical harmonic expansion of the Earth's topography (degree l) (Rapp 1989). The straight line is the dependence of S on k for a Brownian walk obtained from Eq. (2) taking $\beta=2$.

analysis. For a self-affine fractal a spectral analysis results in a power-law relation between the spectral power density S and wave number k (Turcotte, 1997)

$$S = Ck^{-\beta}. \tag{3}$$

For a white-noise time series $\beta=0$ and for a Brownian-walk time series $\beta=2$ (Turcotte, 1997). Spectral expansions of global topography have been carried out, a result is given in Fig. 2. A good correlation with $\beta=2$ is found, i.e. a Brownian walk. This result is consistent with that given in Eq. (2). Tebbens et al. (2002) have shown that the seaward migration and the recession of a sandy coastline is well approximated by a Brownian walk. We will return to the applicability of the Brownian walk statistics to topography when we discuss sediment deposition in Section 5.

3. Drainage networks

Quantification of drainage networks resulted in the Horton–Strahler ordering and power-law scaling. Mandelbrot (1982) pointed out that this power-law scaling is fractal. It is a standard practice to use the Strahler (1957) ordering system. When two like-order streams meet they form a stream with one higher order than the original. Thus, two first-order streams combine to form a second-order stream, two second-order streams combine to form a third-order stream, and so forth. The bifurcation ratio R_B is defined by

$$R_B = \frac{N_i}{N_{i+1}}, \tag{4}$$

where N_i is the number of streams of order i. The length–order ratio R_r is defined by

$$R_r = \frac{r_i}{r_{i+1}}, \tag{5}$$

where r_i is the length of streams of order i; R_B and R_r are found to be nearly constant for a range of stream orders in a drainage basin (Horton, 1945). From Eq. (1) the fractal dimension of a drainage network is

$$D = \frac{\ln(N_i/N_{i+1})}{\ln(r_i/r_{i+1})} = \frac{\ln R_B}{\ln R_r}. \tag{6}$$

The fractality of drainage networks was one of the earliest examples of fractal behavior given by Mandelbrot (1982). Pelletier (1999) has carried out detailed studies of seven drainage networks. He found $R_B=4.6$, $R_L=2.2$ and $D=1.99$ to a good approximation. Three examples of these drainage networks are given in Fig. 3.

While the applicability of Horton–Strahler scaling is certainly of interest, it does not discriminate between alternative models. Many models have been proposed for drainage networks that satisfy this scaling (Rodriguez-

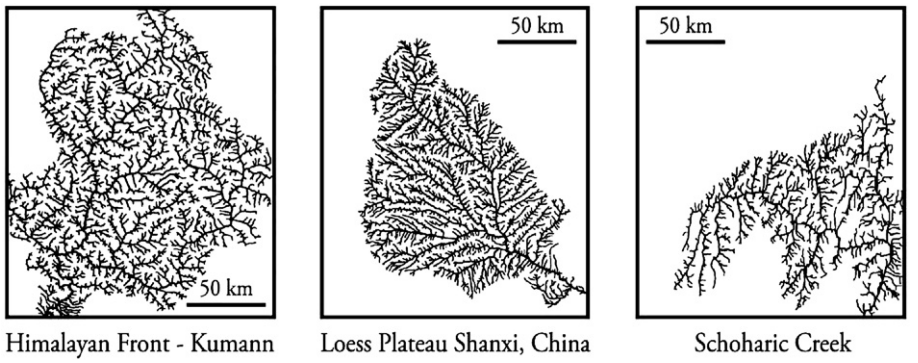

Fig. 3. Three examples of typical drainage networks (after Pelletier, 1999).

Iturbe and Rinaldo, 1997). A major advance in the quantification of drainage networks was made by Tokunaga (1978, 1984, 1994). This author was the first to recognize the importance of side branching; that is some first-order streams intersect second-order, third-order, and all higher-order streams. Similarly, second-order streams intersect third-order and higher-order streams and so forth. To classify side branching Tokunaga (1978, 1984, 1994) extended the Strahler (1957) ordering system. A first-order branch intersecting a first-order branch is denoted "11" and the number of such branches is N_{11}; a first-order branch intersecting a second-order branch is denoted "12" and the number of such branches is N_{12}; a second -order branch intersecting a second-order branch is denoted "22" and the number of such branches is N_{22} and so forth. The total number of streams of order i, N_i, is related to the N_{ij} by

$$N_i = \sum_{j=1}^{n} N_{ij}, \tag{7}$$

for a fractal tree of order n. A deterministic fractal tree with side branching is illustrated in Fig. 4. At each level the primary branch, say 33, has binary branching, two 22 branches, and one 23 side branch. This simple branching structure can be extended to all orders. This is the basic concept of a generator for a fractal construct (Turcotte and Newman, 1996, Newman et al., 1997).

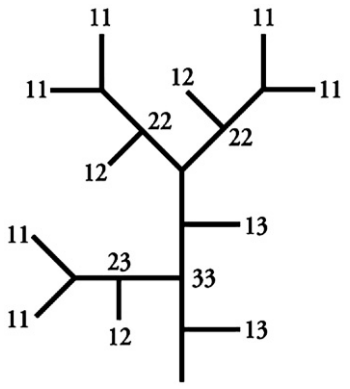

Fig. 4. Example of a binary self-similar fractal tree with side branches.

The branch numbers N_{ij}, $i<j$, constitute a square upper-triangle matrix. This formulation is illustrated in Fig. 5A, the branch-number matrix for the drainage network, illustrated in Fig. 4, is also given in Fig. 5A. For this example the primary branch 33 has two primary second-order branches $N_{22}=2$, one second-order side branch $N_{23}=1$, and two first-order side branches $N_{13}=2$. This class of fractal trees can also be quantified in terms of branching ratios T_{ij}, which are the average number of branches of order i joining branches of order j. Branching ratios are related to branch numbers by

$$T_{ij} = \frac{N_{ij}}{N_i}. \tag{8}$$

Again the branching ratios T_{ij} constitute a square, upper-triangle matrix. This formulation is illustrated in Fig. 5B, the branching-ratio matrix for the drainage network illustrated in Fig. 4 is also given in Fig. 5B. For this example three second-order branches occur so that $N_2=3$. Each of these have a first-order side branch so $N_{12}=3$ and from Eq. (8) $T_{12}=1$.

A

$$\begin{aligned} N_{11} + N_{12} + N_{13} &= N_1 \quad & 6 + 3 + 2 &= 11 \\ N_{22} + N_{23} &= N_2 & 2 + 1 &= 3 \\ N_{33} &= N_3 & 1 &= 1 \end{aligned}$$

B

$$\begin{aligned} T_{12} + T_{13} \quad & 1 \quad 2 \\ T_{23} \quad & 1 \end{aligned}$$

Fig. 5. (A) Illustration of the branch-number matrix for the fractal tree illustrated in Fig. 4. (B) Illustration of the branching-ratio matrix for the fractal tree illustrated in Fig. 4.

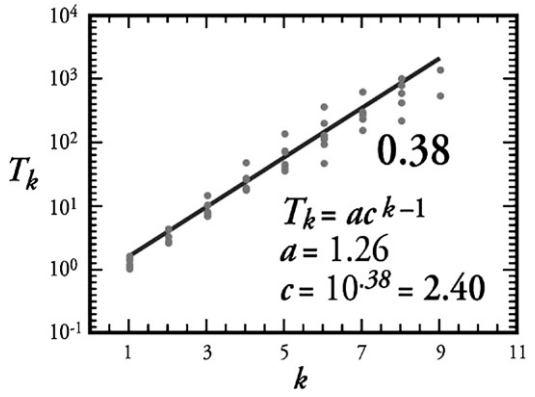

Fig. 6. Dependence of the Tokunaga ratio T_k on the order difference k for the river networks considered by Pelletier (1999).

Tokunaga (1978, 1984, 1994) also introduced a more restricted class of self-similar, side-branching trees by requiring self-similarity of side branching. We define the self-similar Tokunaga fractal trees to be the subset of trees for which $T_{i,\ i+k} = T_k$ where T_k is a branching ratio that depends on k but not on i. In addition it is required that T_k have a power-law dependence on k

$$T_k = T_{i,i+k} = ac^{k-1}. \tag{9}$$

This is now a two parameter family of trees and we will define fractal trees in this class to be Tokunaga trees. For the fractal tree illustrated in Fig. 4, $a = 1$ and $c = 2$.

The dependence of the Tokunaga ratios T_k on the order difference k for the river networks studied by Pelletier (1999) is given in Fig. 6. The self-similar Tokunaga scaling, given by Eq. (8), appears to be a reasonable approximation, taking $a = 1.26$ and $c = 2.4$. The Tokunaga scaling of river networks has also been given by Peckham (1989). Applications of Tokunaga scaling in biology have been studied by Turcotte et al. (1998) and Pelletier and Turcotte (2000). Any classification study of the river networks should certainly consider the side-branching statistics. The Tokunaga scaling provides an important test of any proposed model.

4. Diffusion-limited aggregation (DLA)

Although the application of the Tokunaga side-branching statistics to the river networks has been convincingly demonstrated (Peckham, 1989, Pelletier, 1999), the fundamental question is why? A number of numerical simulations, proposed by statistical physicists, have been shown to have remarkable scaling properties. An example is the concept of diffusion-limited aggregation (DLA), introduced by Witten and Sander (1981). They considered a grid of points on a two-dimensional lattice and placed a seed particle near the center of the grid. An accreting particle was randomly introduced on a "launching" circle and was allowed to follow a random path until: i) it accreted to the growing cluster of particles by entering a grid point adjacent to the cluster or ii) until it wandered across a larger "killing" circle. The resulting sparse, tree-like structure has been taken as an excellent representation of the dendritic growth patterns found in nature and in industrial applications (Fowler, 1990). Ossadnik (1992) has considered the branching statistics of 47 DLA clusters each with 10^6 particles. On average the networks were 11th order fractal trees. The average bifurcation ratio for the clusters was found to $R_B = 5.15$ and the average length-order ratio $R_r = 2.86$, from Eq. (1) the corresponding fractal dimension is $D = 1.56$. The concept of Tokunaga self-similar side branching had been independently introduced into the physics literature by Vannimenus and Viennot (1989). Using their approach Ossadnik (1992) showed that the DLA clusters satisfy the Tokunaga scaling, given in Eq. (8), with $c = 2.7$.

Although the DLA model produces Tokunaga scaling, the network is too sparse to be representative of drainage networks. A modification of the DLA model that does produce networks that are statistically identical to drainage networks was introduced by Masek and Turcotte (1993). Again, a square grid of sites was considered. A number of seed particles were placed along one or more boundaries of a square region. Additional particles were added to randomly selected unoccupied sites in the interior of the grid. The particles were allowed to randomly "walk" through the grid until they reached a site adjacent to the growing network. The resulting network is fractal, typically with $D \approx 1.85$. This modified DLA network also satisfies the Tokunaga side branching statistics with $c = 2.5$.

The modified DLA model can be considered to be analogous to the headward migration of an evolving drainage network into a plateau. "Precipitons" of rain water randomly migrate across the plateau until they reach the river network, and cause headward migration. The concept of migrating "precipitons" was introduced in a model for landform evolution by Chase (1992).

5. Depositional processes

As discussed above, a robust feature of landforms is that the scaling statistics are well approximated by a Brownian walk along linear tracks. A simple model illustrates the creation of the Brownian topography (Pelletier and Turcotte, 1997). Consider a linear set of sites on which "particles" are randomly dropped. If the

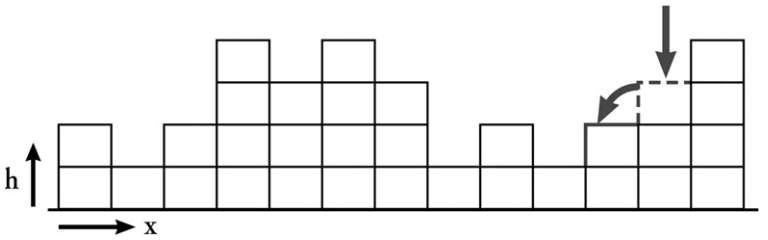

Fig. 7. Illustration of the sediment deposition model. At each time step a site is chosen randomly and a "particle" is dropped on that site. If an adjacent site is lower, the particle is moved to that site as shown.

randomly selected site on which a particle falls is lower (has fewer "particles") than its adjacent sites, the particle remains there. If either adjacent site is lower, the particle is moved to that site. This model is illustrated in Fig. 7. Fig. 8 illustrates a surface produced by the model with a lattice size of 1024. The simulation was run for some time to build up a rough surface. Fig. 9 shows the average power spectrum of the surfaces produced by 50 independent simulations. The power spectrum is proportion to k^{-2}, indicating that the surface is statistically the same as a Brownian walk.

Fig. 10, shows the variations in surface elevation (subtracted from the mean height of the surface) at the central site of our simulation. Fig. 11 gives the average power spectrum of the difference from the mean height of the central site produced in 50 simulations. The power spectrum is proportional to $f^{-3/2}$. As recognized by Family (1986), a continuous version of the discrete model is provided by a one-dimensional diffusion equation with a Gaussian white noise term:

$$\frac{\partial h(x,t)}{\partial t} = D\frac{\partial^2 h(x,t)}{\partial x^2} + \mu(x,t), \qquad (10)$$

where $\mu(x,t)$ is the Gaussian white noise. This equation represents a model in which channels avulse randomly in time and in space across the alluvial plain and the sediment transport is governed by the diffusion equation. This equation and the variants of it have been studied extensively in physics (where it is known as the linear Langevin equation or the Edwards–Wilkinson equation) as a model for the growth of surfaces with random deposition and subsequent diffusion.

The application of the diffusion equation to erosion is known as the Culling model. In this model (Culling, 1960, 1963) the rate of the material transport is assumed to be proportional to the slope. With this assumption, erosion satisfies the heat (diffusive transfer) equation and is controlled by the magnitude of the transfer coefficient, D. From studies of foreland basins Flemings and Jordan (1989) concluded that D is in the range 10^2–10^3 m^2/yr, and from studies of erosion as a driving mechanism for mountain growth Avouac and Burov (1996) conclude that D is in the range 10^3–10^4 m^2/yr. Solutions of the heat equation have been successful in explaining the morphology of alluvial fans, propogating river deltas, and eroding fault scarps (Wallace, 1977, Nash, 1980a,b, Begin et al., 1981, Gill, 1983a,b, Hanks

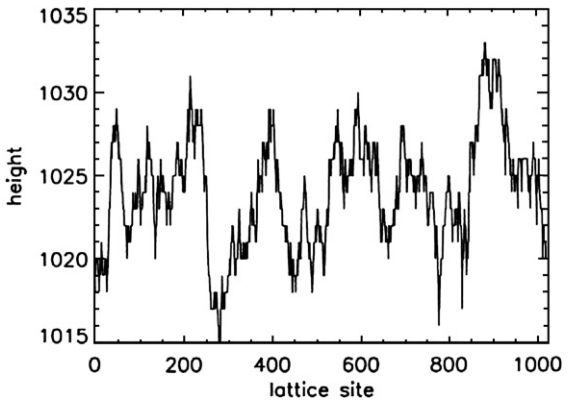

Fig. 8. Surface constructed from the depositional model on a 1024 grid.

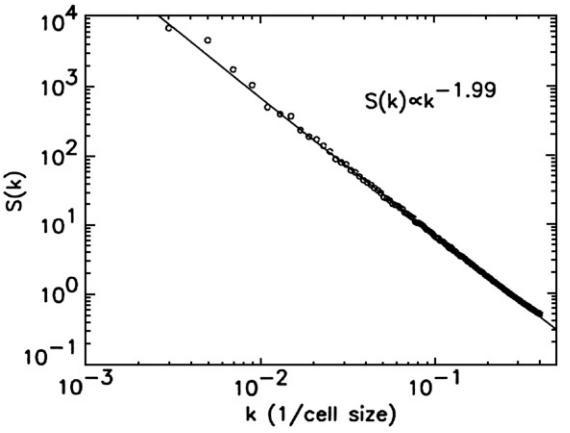

Fig. 9. Average power spectrum of the surfaces constructed from 50 independent simulations on a 1024 grid as function of the wave number k. An exponent of 2 corresponds to a Brownian walk.

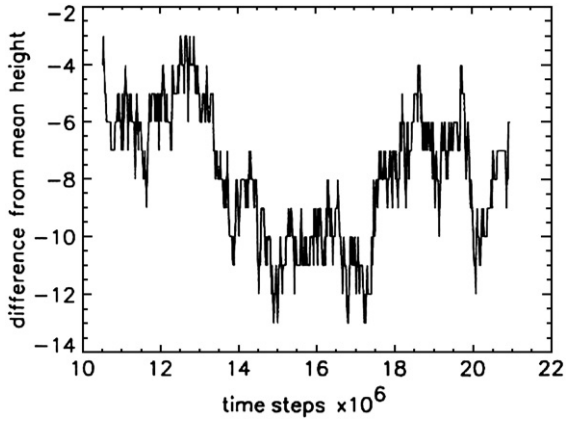

Fig. 10. Difference from the mean height of the central site on the lattice as a function of the time step.

et al., 1984, Kenyon and Turcotte, 1985, Hanks and Wallace, 1985, Hanks and Andrews, 1989).

The deposition model, based on a white noise driver for the Culling model, gives the Brownian walk behavior associated with landforms. The deposition model given above can also be used to model rates of deposition and the completeness of the sedimentary record. The nondimensional height of topography, $h\sigma/D$ (D diffusion coefficient, σ standard deviation of the white noise), is given in Fig. 12 as a function of nondimensional time, $t\sigma^2/D$ for a nondimensional subsidence rate σ/η (η velocity of subsidence).

This result is the same as that given in Fig. 10 with a constant velocity deposition superimposed. It is then assumed that in periods when the rates of sedimentation are greater than the rate of subsidence the topography is

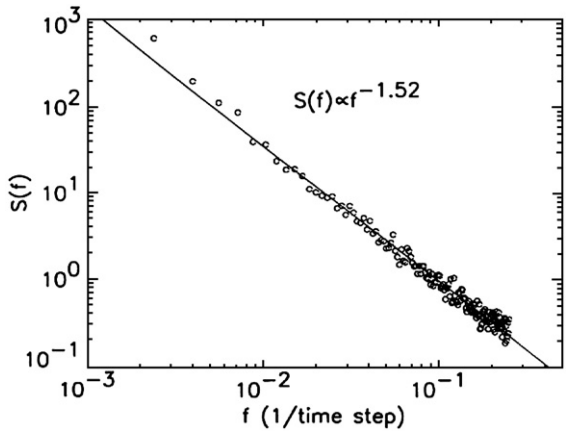

Fig. 11. Average power spectrum of the difference from the mean height of the central site for 50 independent simulations as a function of frequency in time steps −1. The power spectrum is proportional to $f^{-3/2}$.

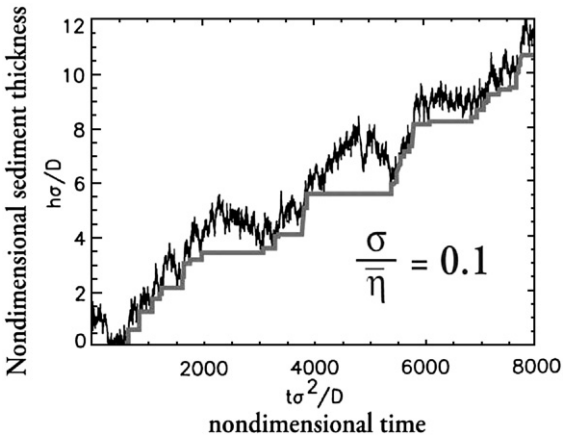

Fig. 12. The nondimensional thickness of sediments $h\sigma/D$ in a sedimentary basin as a function of nondimensional time $t\sigma^2/D$ for a sequence in which the ratio of the standard deviation δ to the mean subsidence rate η is 0.1. Also illustrated is the record of deposition if sediments are removed (eroded) when the deposition rate exceeds the subsidence rate. The horizontal lines are the resulting unconformities.

eroded and gives uniformities as illustrated in Fig. 12. The result is a reduction in the mean rate of sedimentation R as the time interval T increases. This dependence is given in Fig. 13, the nondimensional deposition rate R/n is given as a function of the nondimensional time interval $T\sigma^2/D$. The nondimensional rate of sedimentation has a power-law dependence on the nondimensional time span with exponent −3/4.

Sadler (1981) has compiled measurements of the rates of fluvial sedimentation from the geological literature with time scales of minutes to 100 million years. His data (Sadler and Strauss, 1990) are plotted in Fig. 14. A least-squares linear fit to the logarithms (base 10) of the data yields a slope of −0.75. This result is in

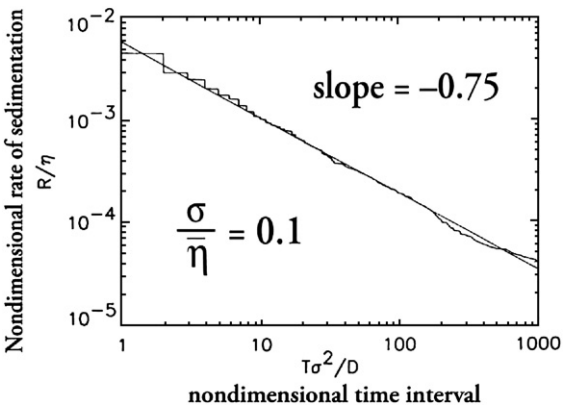

Fig. 13. Average rate of sedimentation, R/η, as a function of the nondimensional time span, $T\sigma^2D$, for the sediment column of Fig. 12.

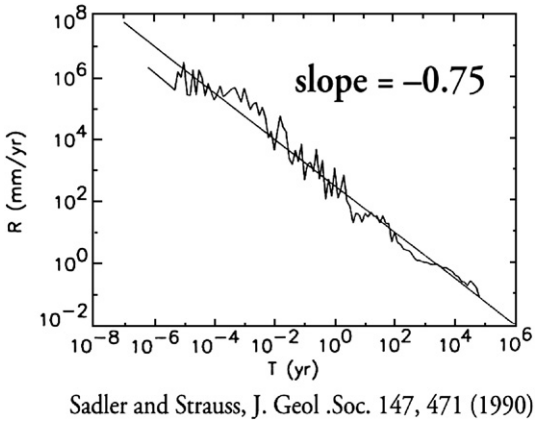

Fig. 14. Observed sedimentation rates as a function of time span, from Sadler and Strauss (1990). The data have been binned logarithmically to obtain a uniform distribution of points in log–log space. A least-squares linear fit to the logarithms of the data yields a slope of −3/4.

agreement with the analysis of the model given in Fig. 13.

These results can also be obtained from theoretical fractal relations. Fractional Brownian walks have the property that the standard deviation of the time series has a power-law dependence on time with a fractional exponent called the Hausdorff measure, Ha:

$$\sigma_h \sim T^{\mathrm{Ha}}. \tag{11}$$

The power spectral exponent of a time series and its Hausdorff measure have been related theoretically by (Turcotte, 1997)

$$\mathrm{Ha} = \frac{\beta - 1}{2}. \tag{12}$$

As seen in Fig. 11, $\beta = 3/2$ is a good approximation for the deposition model. And from Eqs. (11) and (12), $\mathrm{Ha} = 1/4$ and $\sigma_h \sim T^{1/4}$. Taking the rate of sedimentation R to be the ratio of σ_h to T results in

$$R = \frac{\sigma_h}{T} \sim T^{-3/4}. \tag{13}$$

This is in good agreement with the results given in Figs. 13 and 14. Details of this analysis have been given by Pelletier and Turcotte (1997).

6. Discussion

A fundamental objective is to understand the origin of landforms and drainage networks. Clearly a wide range of landforms exist. Some are very deterministic and can be understood in terms of classical applied mathematics. We give three examples. The first example is the morphology of ocean ridges. This is explained by conductive cooling of a half space, thermal contraction, and isostacy (Turcotte and Schubert, 2002, pp. 153–161). The second example of alluvial fans and propagating river deltas was discussed in Section 4 using the Culling model for erosion. A third example is the remarkably symmetric structure of volcanic landforms, i.e. Mount Fuji. This structure can be explained by the balance between gravity and flow resistance through a porous matrix (Lacey et al., 1981, Turcotte and Schubert, 2002, pp. 387–390).

The focus of this paper has been on the more complex aspects of landforms and drainage networks. The basis of quantification is the fractal scaling. Many fundamental questions remain concerning this scaling. Fractal (power-law) scaling is the only scaling that is scale invariant and it is widely accepted that many geological forms are scale invariant. Fractal scaling is ubiquitous in all branches of science and engineering. Many attempts have been made to model this behavior. The most successful have involved simulations. A classic example is DLA. We have discussed in some detail the association of DLA with the fractal structure of drainage networks. The generation of self-affine fractal surfaces is also widely recognized, but has not been easy to generate. The use of stochastic differential equations, i.e. the Langevin equation, has been the most successful. We have shown how this approach can give the Brownian motion behavior of landforms and the deposition structure of sedimentary layering.

7. Conclusions

Landforms and drainage networks satisfy fractal scaling laws in a variety of ways. For landforms, examples include coastlines, topography along linear tracks, and lakes. For drainage networks the branching statistics are fractal both in terms of the Horton–Strahler primary branching and the Tokunaga side branching. Explanations for this behavior come from several models developed by statistical physicists. For landforms the applicable model is the Langevin equation. The Langevin equation is the heat equation with a stochastic (white) noise driver. The applicability of the heat equation to deposition is known as the Culling model.

Fractal branching statistics are generated by the diffusion-limited aggregation (DLA) model. This model also satisfies the Tokunaga self-similar side-branching statistics. A modified version of the DLA model is in quantitative agreement with the statistics of drainage networks.

References

Ahnert, F., 1984. Local relief and height limits of mountain ranges. Am. J. Sci. 284, 1035–1055.

Avouac, J.P., Burov, E.B., 1996. Erosion as a driving mechanism of intracontinental mountain growth. J. Geophys. Res. 101, 17,747–17,769.

Barabasi, A.L., Stanley, H.E., 1993. Fractal Concepts in Surface Growth. Cambridge University Press, Cambridge.

Begin, Z.B., Meyer, D.F., Schumm, S.A., 1981. Development of longitudinal profiles of alluvial channels in response to base level lowering. Earth Surf. Proc. Landf. 6, 49–68.

Chase, C.G., 1992. Fluvial landsculpting and the fractal dimension of topography. Geomorphology 5, 39–57.

Culling, W.E.H., 1960. Analytical theory of erosion. J. Geol. 68, 336–344.

Culling, W.E.H., 1963. Soil creep and the development of hillside slopes. J. Geol. 71, 127–161.

Family, F., 1986. Scaling of rough surfaces: effects of surface diffusion. J. Phys. A 19, L441–L446.

Flemings, P.B., Jordan, T.E., 1989. A synthetic stratigraphic model of foreland basin development. J. Geophys. Res. 94, 3851–3866.

Fowler, A.D., 1990. Self-organized mineral textures of igneous rocks: the fractal approach. Earth-Sci. Rev. 29, 47–55.

Gill, M.A., 1983a. Diffusion model for aggrading channels. J. Hydraul. Res., 21, 355–367.

Gill, M.A., 1983b. Diffusion model for degrading channels. J. Hydraul. Res., 21, 368–378.

Hanks, T.C., Andrews, D.J., 1989. Effect of far-field slope on morphologic dating of scarplike landforms. J. Geophys. Res., 94, 565–573.

Hanks, T.C., Wallace, R.E., 1985. Morphological analysis of the Lake Lahontan shoreline and beachfront fault scarps, Pershing County, Nevada. Bull. Seis. Soc. Am., 75, 835–846.

Hanks, T.C., Bucknam, R.C., Lajoie, K.R., Wallace, R.E., 1984. Modification of wave-cut and faulting-controlled landforms. J. Geophys. Res., 89, 5771–5790.

Hewett, T.A., 1986. Fractal distributions of reservoir heterogeneity and their influence on fluid transport. Soc. Petrol. Eng. Paper 15386.

Horton, R.E., 1945. Erosional development of streams and their drainage basins; hydrophysical approach to quantitative morphology. Geol. Soc. Am. Bull. 56, 275–370.

Kenyon, P.M., Turcotte, D.L., 1985. Morphology of a delta prograding by bulk sediment transport. Geol. Soc. Am. Bull., 96, 1457–1465.

Lacey, A., Ockendon, J.R., Turcotte, D.L., 1981. On the geometrical form of volcanoes. Earth Planet. Sci. Let. 54, 139–143.

Mandelbrot, B., 1967. How long is the coast of Britain? Statistical self-similarity and fractional dimension. Science 156, 636–638.

Mandelbrot, B., 1982. The Fractal Geometry of Nature. Freeman, San Francisco.

Masek, J.G., Turcotte, D.L., 1993. A diffusion-limited aggregation model for the evolution of drainage networks. Earth Planet. Sci. Let. 119, 379–386.

Meybeck, M., 1995. Global distribution of lakes, In: Lerman, A., Imboden, D.M., Gat, J.R. (Eds.), Physics and Chemistry of Lakes, 2nd ed. Springer-Verlag, Berlin, pp. 1–35.

Molz, F.J., Rajaram, H., Lu, S., 2004. Stochastic fractal-based models of heterogeneity in subsurface hydrology: origins, applications, limitations, and future research questions. Rev. Geophys 42, RG1002.

Nash, D.B., 1980a. Morphological dating of degraded normal fault scarps. J. Geol. 88, 353–360.

Nash, D., 1980b. Forms of bluffs degraded for different lengths of time in Emmet County, Michigan, U.S.A. Earth Surf. Proc. Landf. 5, 331–345.

Newman, W.I., Turcotte, D.L., Gabrielov, A.M., 1997. Fractal trees with side branching. Fractals 5, 603–614.

Ossadnik, P., 1992. Branch order and ramification analysis of large diffusion limited aggregation clusters. Phys. Rev. A 45, 1058–1066.

Peckham, S.D., 1989. New results for self-similar trees with applications to river networks. Water Resour. Res. 31, 1023–1029.

Pelletier, J.D., 1999. Self-organization and scaling relationships of evolving river networks. J. Geophys. Res. 104, 7259–7375.

Pelletier, J.D., Turcotte, D.L., 1997. Synthetic stratigraphy with a stochastic diffusion model of fluvial sedimentation. J. Sed. Res. 67, 1060–1067.

Pelletier, J.D., Turcotte, D.L., 2000. Shapes of river networks and leaves: are they statistically similar? Phil. Trans. Roy. Soc. B 355, 307−311.

Rodriquez-Iturbe, I., Rinaldo, A., 1997. Fractal River Basins. Cambridge University Press, Cambridge.

Sadler, P.M., 1981. Sediment accumulation rates and the completeness of the stratigraphic record. J. Geol. 89, 569–584.

Sadler, P.M., Strauss, D.J., 1990. Estimation of completeness of stratigraphical sections using empirical data and theoretical models. J. Geol. Soc. London 147, 471–485.

Strahler, A.N., 1957. Quantitative analysis of watershed geomorphology. Am. Geophys. Un. Trans. 38, 913–920.

Tebbens, S.F., Burroughs, S.M., Nelson, E.E., 2002. Wavelet analysis of shoreline change on the Outer Banks of North Carolina: an example of complexity in the marine sciences. Proc. Nat. Acad. Sci. 99, 2554–2560.

Tokunaga, E., 1978. Consideration on the composition of drainage networks and their evolution. Geogr. Rep. Tokyo Metrop. Univ. 13, 1–27.

Tokunaga, E., 1984. Ordering of divide segments and law of divide segment numbers. Jap. Geomorph. Un. 5, 71–78.

Tokunaga, E., 1994. Selfsimilar natures of drainage basins. In: Takaki, R. (Ed.), Research of pattern formation. KTK Scientific Publishers, Tokyo, pp. 445–468.

Turcotte, D.L., 1997. Fractals and Chaos in Geology and Geophysics, 2nd ed. Cambridge University Press, Cambridge.

Turcotte, D.L., 2006. Modeling geocomplexity: “a new kind of science. In: Manduca, C.A., Mogk, D.W. (Eds.), Earth and Mind: How Geologists Think and Learn about the Earth. Geological Society of America, Boulder, CO, pp. 39–50.

Turcotte, D.L., Newman, W.I., 1996. Symmetries in geology and geophysics. Proc. Natl. Acad. Sci. 93, 14295–14300.

Turcotte, D.L., Schubert, G., 2002. Geodynamics, 2nd ed. Cambridge University Press, Cambridge.

Turcotte, D.L., Pelletier, J.D., Newman, W.I., 1998. Networks with side branching in biology. J. Theor. Biol. 193, 577–592.

Vannimenus, J., Viennot, X.G., 1989. Combinatorial tool for the analysis of ramified patterns. J. Stat. Phys. 54, 1529–1538.

Voss, R.F., 1989. Random fractals: self affinity in noise, music, mountains, and clouds. Physica D 38, 362–371.

Wallace, R.E., 1977. Profiles and ages of young fault scarps, north–central Nevada. Geol. Soc. Bull., 88, 1267–1281.

Witten, T.A., Sander, L.M., 1981. Diffusion-limited aggregation a kinetic critical phenomenon. Phys. Rev. Let. 47, 1400–1403.